Am J Cancer Res 2023;13(11):5577-5589
www.ajcr.us /ISSN:2156-6976/ajcr0150417

Original Article

Detection of CSTF2 by nano fluorescent probe and its correlation with malignant biological characteristics in liver cancer

Zhongmin Jiang[1,2,3*], Xiaozhi Liu[2,3*], Yongqing Deng[2,4], Duojierenqing[2,4], Renqingcuo[2,5], Wenhan Wu[2,3,6,7], Wei Meng[2,8,9], Zhijiang Shao[2,6]

[1]Department of Pathology, Tianjin Fifth Central Hospital, Tianjin 300450, P.R. China; [2]High Altitude Characteristic Medical Research Institute, Huangnan Tibetan Autonomous Prefecture People's Hospital, Huangnan 811399, Qinghai, P.R. China; [3]Tianjin Key Laboratory of Epigenetic for Organ Development of Preterm Infants, Tianjin Fifth Central Hospital, Tianjin 300450, P.R. China; [4]Department of General Surgery, Huangnan Tibetan Autonomous Prefecture People's Hospital, Huangnan 811399, Qinghai, P.R. China; [5]Department of Infectious Diseases, Huangnan Tibetan Autonomous Prefecture People's Hospital, Huangnan 811399, Qinghai, P.R. China; [6]Department of General Surgery, Tianjin Fifth Central Hospital, Tianjin 300450, P.R. China; [7]Department of General Surgery, Peking University First Hospital, Beijing 100034, P.R. China; [8]Department of Orthopedics, Huangnan Tibetan Autonomous Prefecture People's Hospital, Huangnan 811399, Qinghai, P.R. China; [9]Department of Orthopedics, Tianjin Medical University General Hospital Binhai Hospital, Tianjin 300480, P.R. China. [*]Equal contributors.

Received March 29, 2023; Accepted September 23, 2023; Epub November 15, 2023; Published November 30, 2023

Abstract: To develop a novel nano DNA fluorescent probe for in situ detection of CSTF2 in liver cancer (LC) and study its correlation with the development of LC, we developed nano-TiO_2-DNA fluorescent probe which can bind with CSTF2 in LC samples with high efficiency. The detection process of CSTF2 did not involve the use PCR technology, and the concentration of CSTF2 can be directly observed by fluorescence intensity. This probe exhibited excellent physicochemical properties in ethyl alcohol at -20°C and could directly and selectively permeate into Hep-3B cells. By using CSTF2 Nano-TiO_2-DNA probe, we found that the CSTF2 level increased greatly in LC tissue and cells, and high CSTF2 level was closely associated with high levels of tumor markers and poor prognosis in LC patients. After transfection, CSTF2 was overexpressed or silenced in Hep-3B cells, and we find that high CSTF2 level effectively increased the activity and invasion of Hep-3B cells and reduced their apoptosis. Furthermore, high CSTF2 level significantly increased the tumor volume and weight in mice models by activating PI3K/AKT/mTOR signal pathway. Therefore, CSTF2 can serve as an early biomarker of LC and a novel potential target for its treatment.

Keywords: TiO_2-DNA probe, CSTF2, in situ, liver cancer, prognosis

Introduction

Liver cancer (LC), with a five-year survival rate of 10%-15%, has been considered to be one of the most common gastrointestinal tumors in China [1]. Chronic viral hepatitis is an important risk factor for LC, and there are about 90 million patients with chronic hepatitis B in China, which leads to a high incidence of LC [2]. In addition, the onset of LC is often insidious, with inconspicuous symptoms in the early stage. As a result, patients are often diagnosed in advanced stages, leading to missed opportunity for optimal treatment [3]. In advanced stages, LC exhibits rapid progression and concurrent emergence of a variety of complications, rendering surgical treatment unfeasible and affecting the efficacy of chemotherapy [4]. Therefore, exploring more sensitive biomarkers for the early diagnosis of LC is of positive significance to improve patients' prognosis. This effort also supports the determination of novel therapeutic targets, so as to inhibit the rapid progression of LC.

With the development of molecular genetics technology, increasing genes, such as ZEB2 and SP1, have been found to be related to the occurrence of cancers [5, 6]. The up-regulation of their expression can greatly increase the activity and invasiveness of cancer cells, leading to poor prognosis in cancer patients. Therefore, studying the pathogenesis and progression of LC on a gene level can provide a new direction for the early diagnosis and treatment of LC. Recently, a study found that the shortening of mRNA 3'-UTR was closely related to the upregulation or activation of oncogene, which is an important factor contributing to the continuous progression of tumors [7]. The shortening of mRNA 3'-UTR may lead to the deletion of complementary binding sites for miRNA, which facilitates escaping miRNA-mediated targeted inhibition and activating related oncogenes [8]. For example, in human breast cancer, lung cancer, colorectal cancer, and kidney cancer, researchers found that tumor with shorter mRNA 3'-UTR tended to be more aggressive, and the patients are associated with poorer prognosis [9-11]. Cleavage stimulation factor subunit 2 (CSTF2), as one of the three subunits of CSTF complex, is positively correlated with the shortening trend of mRNA 3'-UTR [12]. This suggests that CSTF2 plays an important regulatory role in tumor progression. For example, the upregulation of CSTF2 can contribute to the carcinogenic activity of hepatocellular carcinoma [13]. Accordingly, it is reasonable to assume that CSTF2 may promote the development of LC, but its specific mechanism remains inadequately investigated. Therefore, studies on abnormal expression and mechanism of CSTF2 in LC may provide a new research direction.

In order to better understand the role of CSTF2 in LC, enhancing its detection accuracy in LC tissues is pivotal. Traditionally, the pathological diagnosis of LC usually depends on the second-generation sequencing technology. Although the target cDNA can be amplified by conventional qPCR, the quantity of tissue samples obtained by puncture is often limited, which may affect the reliability of the results. Hence, a relatively simple and intuitive detection approach is needed to improve the accuracy and make up for the shortcomings of conventional qPCR. Here, we created a synthetic nanostructured DNA probe called nano-TiO_2-DNA probe. The combination of nano-TiO_2-DNA probe and target sequence has high efficiency and specificity. The coupled fluorescent group's ability to restore fluorescence post-binding enables direct and intuitive detection of small molecules in situ. This advancement holds potential for expediting clinical screening, especially in scenarios involving small samples like biopsy tissues. In addition, when combined with TiO_2 nanoparticle (NP), the DNA probe gains enhanced penetration into tissues and cells, effectively promoting the combination with the target sequence and thereby improving the detection sensitivity [14, 15]. To our knowledge, there are few studies on utilizing DNA probes to assess CSTF2 levels and exploring the association between CSTF2 and malignant biological features in LC. Therefore, this study aimed to examine CSTF2 levels in LC and their correlation with LC progression.

Materials and methods

Physicochemical properties test of nano-TiO_2

TiO_2 NP (13463-67-7, Sigma-Aldrich, MO, USA) was used as the vector of nano DNA probe in this study. Firstly, we tested its binding ability to LC cells. Nano TiO_2-Cy5 (ab6564, Abcam, USA) was mixed with Hep-3B cells (CL-010, Procell, Wuhan, China) and stained by Alexa Fluor® 405 (ab175652, Abcam). After 1-h incubation, the fluorescence intensity was tested. Secondly, we determined the optimal preservation medium and temperature for the nano DNA fluorescent probe, ensuring its maximal solubility and robust stability in the medium. TiO_2-FITC was dissolved in distilled water, NaOH, formic acid, methyl alcohol, and ethyl alcohol. The fluorescence intensity of the sediment was observed after the solutions were placed in dark for 24 h. After determining the optimal medium, TiO_2-FITC solution was stored under different temperatures, including -60°C, -20°C, 10°C, 37°C, and 60°C, and the fluorescence intensity of TiO_2 sediment was observed after 24 h. The fluorescence intensity was observed by a confocal microscopy (ZEISS, LSM800). Three sets of experiments were conducted to investigate the stability and permeability of TiO_2, and the average fluorescence intensity of each set was taken.

Preparation of nano-TiO_2-DNA probe

Firstly, we synthesized CSTF2-related oligonucleotides (TCACAGGTGAATGACA-GGAGAGGA).

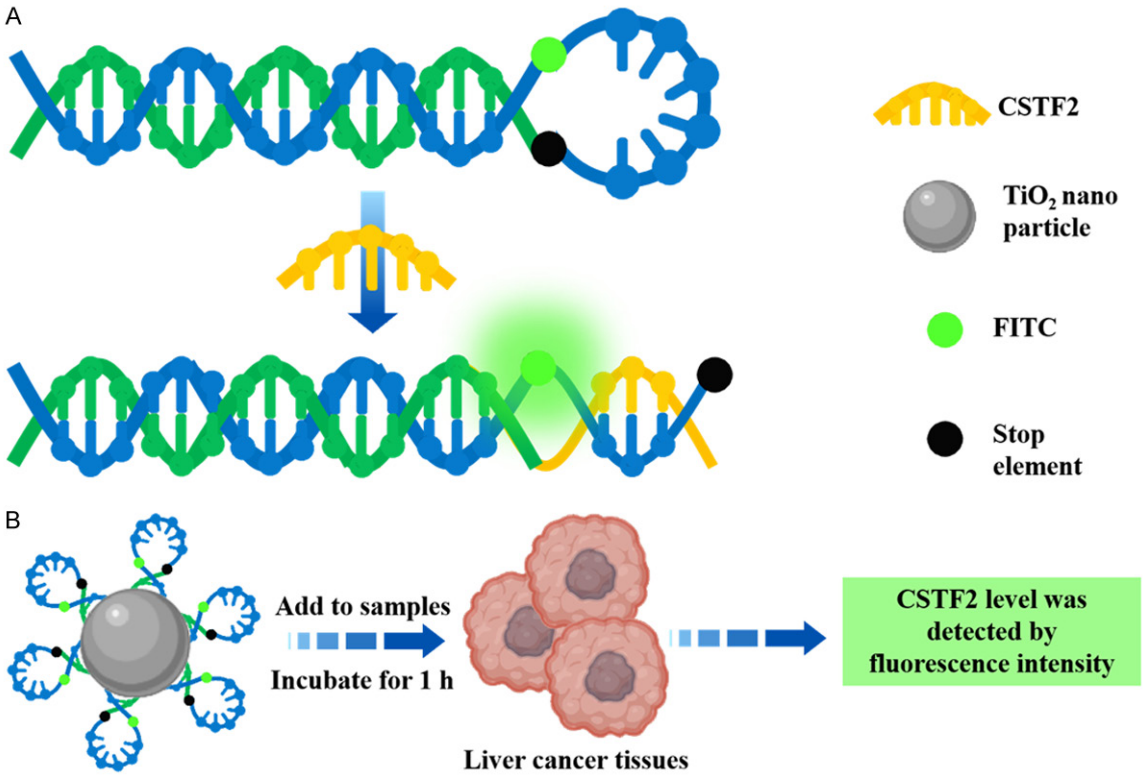

Figure 1. Synthesis principle and workflow of Nano-TiO_2-DNA.

Next, the oligonucleotides were modified with FITC (ab6717, Abcam, USA) to label the beacon by magnetic stirring under 60°C. Then, a non-fluorescent stop beacon was modified on the opposite end of the oligonucleotides by incubating with them in glycerol under 37°C. This interaction allowed the formation of a stem-loop structure by connecting with the CSTF2 sequence, preventing the release FITC fluorescence. Subsequently, CSTF2 DNA probe and TiO_2 NP were dissolved in borate buffer, and the mixture was stirring at 37°C for 12 h, and nano-TiO_2-DNA probe precipitate was obtained by centrifuging at 3000 rpm and then stored at 4°C for later use (**Figure 1**).

Permeability test of nano-TiO_2-DNA probe

Nano DNA probe and nano-TiO_2-DNA probe (stained by Cy5) of CSTF2 were mixed with Hep-3B cells (stained by Alexa Fluor® 405) for infiltration ability test. After 10 min, the fluorescence image was observed by the confocal microscopy. Three permeability experiments were conducted in each group, and the average fluorescence intensity was taken.

Research subjects

LC patients who were treated in Tianjin Fifth Central Hospital from August 2012 to August 2020 and in Huangnan Tibetan Autonomous Prefecture People's Hospital from January 2015 to August 2020 were included as research subjects. Inclusion criteria: (1) patients who were diagnosed for the first time; (2) patients who met the diagnostic criteria of primary LC in *Asian Pacific Association for the Study of the Liver consensus recommendations on hepatocellular carcinoma* [16]; (3) patients who were 18-60 years old; (4) patients with tumor diameter over 2 cm; (5) patients without previous local treatment or chemotherapy. Exclusion criteria: (1) patients with active hepatitis; (2) patients with CNLC stage IV; (3) patients with other malignant tumors; (4) patients with previous history of liver surgery. Following the criteria, a total of 70 patients were included in a LC group, and their liver biopsy specimens were stored in liquid nitrogen and transferred into a medical refrigerator at -80°C. Meanwhile, 49 liver cyst biopsy specimens collected in the same period were used as con-

trols. All the subjects in the study signed an informed consent.

Culture of HL7702 cells and LC cell lines

In this study, we chose normal liver cells HL7702 (CL-0111, Procell), and LC cell lines Hep-3B, HCCLM3 (CL-0278, Procell), and Huh7 (CL-0120) for in vitro experiments. The above cells were cultured in 24-well plates with DMEM (D8537, Merck, Germany) and 10% fetal bovine serum (SV30087.03, HyClone, USA). The cells were placed in a cell incubator (Herocell 180, Shanghai Rundu Biotechnology Co., Ltd.) maintained at a temperature of 37°C and supplemented with 5% CO_2. After 24-hour incubation, the above cells were diluted to a concentration of 4×10^4/mL for later use.

Detection of CSTF2 by nano fluorescence probe

LC and liver cyst specimens stored in the medical refrigerator were taken out to measure the expression levels of CSTF2. The nano DNA probe of CSTF2 was hybridized with the tissue specimens, and the subsequent detection process was shown in above in *Preparation of nano-TiO_2-DNA probe*.

Detection of tumor markers and survival analysis

LC patients were divided into an H-CSTF2 group and an L-CSTF2 group according to the median of CSTF2 level. Their clinical data were collected and the clinicopathological features were comparatively analyzed. In addition, the survival of LC patients was followed up by telephone, WeChat, outpatient visits and home visit, with the end-point event being all-cause death and the secondary event being further progression or relapse. The follow-up period was 24 months and ended in August 2022.

Hep-3B cell transfection

The previous prepared Hep-3B cells were used as studied cell lines and transfected by Lipofectamine 2000. pcDNA-CSTF2-EGFP was used for the overexpression of CSTF2, and si-h-CSTF2 (caccGTGTCCTGAGATGGCTTGTAAGctcgagATTCTCT TCCTCTGTGCGCCG, siB14113-165307-1-5, RiboBio, Guangzhou, China) was used for silencing CSTF2. The sequence of scrambled shRNA was CCGGCAACAAGATGAAGAGCACCAACTCGAGTTGGTGCTCTTCATCTTGTTGTTTTTG. After 6 hours of transfection, Hep-3B cells were divided into three groups, control group without any treatment, H-CSTF2 group, and L-CSTF2 group, and the above cells were cultured for another 24 h. Each group was equipped with three compound wells.

Detection of Hep-3B cell activity in vitro

Hep-3B cell activity was detected by immunofluorescence. The transfected cells were stained by Anti-ki67 (ab15580, Abcam), and FITC was used as secondary antibody. Then, the cell ability was observed by confocal microscope, and the cell density was observed under a differential interference contrast (DIC) microscope (MX8R, Dongguan beitesen Precision Instrument Co., Ltd., China).

Evaluation of Hep-3B cell apoptosis in vitro

After transfection, Hep-3B cell apoptosis was analyzed to evaluate the role of CSTF2. Anti-cleaved caspase3 antibody (ab32042, Abcam, USA) was added to mark apoptotic Hep-3B cells, and Cy3.5 (ab6941, Abcam) was used as secondary antibody. Then, apoptotic cells in each group were detected by the confocal microscope.

Detection of Hep-3B cell migration

In order to detect the migration of Hep-3B cells in each group, wound healing assay was performed. Hep-3B cells of each group were seeded in a 12-well plate with a total cell number of 1×10^4, and each group was equipped with three compound wells. Following the creation of a scratch on the cell layer using a pipette tip, PBS solution was used to remove any remaining Hep-3B cells within the scratch. After an additional 24-h incubation, the migration of Hep-3B cells within the scratch was observed by a microscope (BX53, OLYMPUS, JAPAN), and the total number of migrating chondrocytes was determined.

Establishment of LC mice model

Nine 6-8-week-old male C56BL/6J mice (Jiangsu Jicui Yaokang Biotechnology Co., Ltd., China) weighing 30 g were selected to construct LC animal model. They were randomly divided into

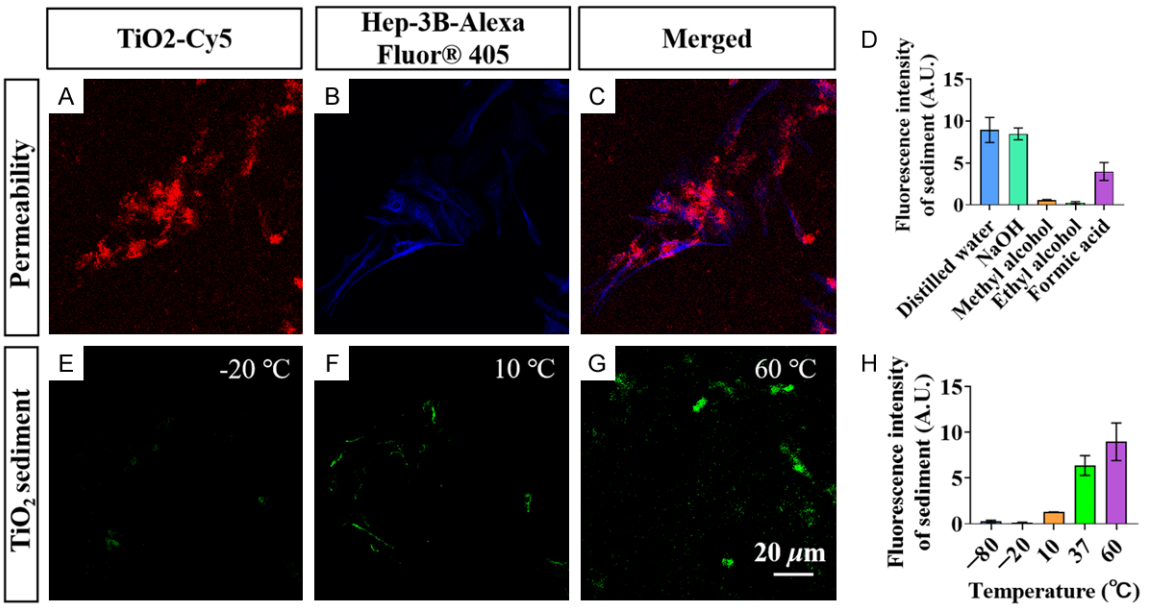

Figure 2. Physicochemical Characteristics of TiO_2 NP. A: Confocal image of TiO_2-FITC. B: Confocal image of Hep-3B cells stained by Alexa Fluor® 405. C: Confocal image of merged TiO_2-FITC and Hep-3B cells. D: Dissolving capacity test of TiO_2. E-G: Confocal image of precipitate TiO_2-FITC after TiO_2-FITC solution at different temperature. H: Quantitative fluorescence precipitates of TiO_2-FITC at different temperature.

a control (n=3), an H-CSTF2 (n=3), and an L-CSTF2 group (n=3). Then, 100-μL transfected Hep-3B cell dilution was injected into the back skin of each mouse. After 14 days, the LC mice model was successfully constructed, and the tumor volume was measured every four days. After 34 days, the above mice were sacrificed to harvest the tumor tissue, and CSTF2 level and weight of tumor tissue were examined. This animal experiment was approved by Tianjin Fifth Central Hospital Laboratory Animal Ethics Committee.

Immunohistochemical analysis

To investigate the role of PI3K/AKT/mTOR pathway in LC progression and CSTF2, the tumor tissue of mice in each group were fixed in 4% formalin for 72 hours and sectioned 5-mm slices. Then, the slices were incubated with anti-PI 3 Kinase p85 beta antibody [EPR18416] (ab180967, Abcam), anti-AKT (phospho T308) antibody (ab38449, Abcam), and anti-mTOR antibody [EPR390(N)] (ab134903, Abcam) at 4°C overnight, and IHC staining was used to analyze the expressions of PI3K, AKT, and mTOR. The fluorescence intensity of the above indexes in each group was observed by a fluorescence spectrophotometer.

Statistical processing

Data were analyzed using SPSS 22.0 and GraphPad Prism7. Categorical variables were expressed as n (%) and tested using the χ^2 test. Continuous variables that conformed to a normal distribution were presented as mean ± standard deviation (SD), and the two-tailed Student's *t*-test was applied to assess the differences between two groups; those did not conform to a normal distribution were presented as median value with interquartile range (IQR), and differences between the two groups were tested using the Mann-Whitney non-parametric test. Person correlation analysis was used to analyze the correlation between CSTF2 and tumor markers. Survival curves were plotted using the Kaplan-Meier curve. Statistical significance was indicated when $P < 0.05$.

Results and discussion

Physicochemical characteristics of TiO_2 NP

The permeability of TiO_2 NP in LC cells plays a key role in improving the permeability of our designed nano fluorescent probe. Obviously, TiO_2 NP could permeate into Hep-3B cells directly (**Figure 2A-C**) and presented effective

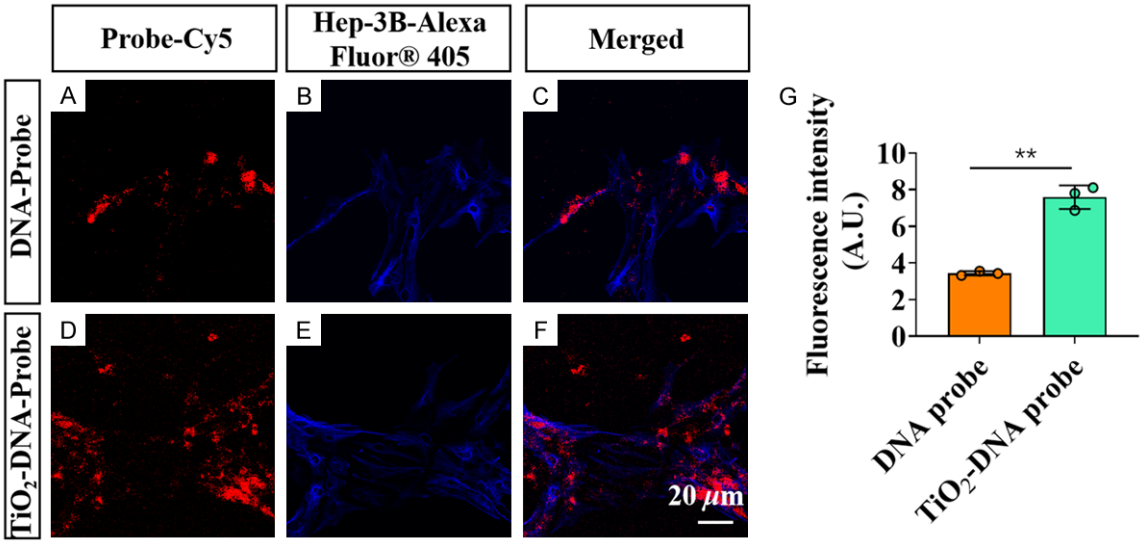

Figure 3. Permeation Capacity Comparison of Nano DNA probe and Nano TiO_2-DNA probe. A-C: Permeability of pure DNA probe in Hep-3B cells. D-F: Permeability of TiO_2 DNA probe in Hep-3B cells. G: Quantitative permeability fluorescence intensity of DNA probe and TiO_2-DNA probe. $^{**}P < 0.01$.

co-localization with Hep-3B cells, as evidenced by confocal image. Besides, TiO_2 could maintain the maximum solubility in methanol and exhibited minimal precipitation after 24 h of standing (**Figure 2D**). Meanwhile, we found the lower the temperature, the better the stability of TiO_2 NP. Therefore, we recommend that nano-TiO_2-DNA probe should be stored under -20°C (**Figure 2E-H**).

Nano TiO_2-DNA probe could better penetrate into Hep-3B cells

To further detect the effect of TiO_2 NP on the permeability of nano fluorescent probe, we observed its permeability in Hep-3B cells. With the help of TiO_2 NP, nano DNA probe could better penetrate into Hep-3B cells (**Figure 3A-F**). Quantitative analysis showed that the fluorescence intensity of TiO_2-DNA probe was higher than that of pure DNA probe (**Figure 3G**).

CSTF2 level was up-regulated in LC tissue

The CSTF2 level was higher in the LC tissue, Hep-3B cells, HCCLM3 cells, and Huh7 cells than that in liver cysts and HL7702 cells (**Figure 4A**, **4B**). In addition, in order to further explore the CSTF2 level in different LC tissue, we grouped LC specimens according to tumor diameter, tumor differentiation, and CNLC grade. It was found that the CSTF2 level increased significantly in the tissue with tumor diameter greater than 5 cm, poor differentiation, and or stage III (**Figure 4C-E**). The above results indicate that CSTF2 is closely related to the progression of LC.

High CSTF2 level was closely related to the clinicopathological characteristics and prognosis of patients

The clinicopathological features of LC patients were evaluated, including age, tumor diameter, lymph node metastasis, CNLC stage, tumor differentiation, and Child-Pugh grade. It was found that there were more patients with large tumor diameter, high lymph node metastasis rate, high CNLC stage, and poor differentiation in the H-CSTF2 group than in the L-CSTF2 group (**Table 1**). Besides, the levels of AFP, CA-199, and PIVKA-II were significantly higher in the H-CSTF2 group (**Table 2**), and the tumor markers were positively correlated with the CSTF2 level (**Figure 5A-C**). As shown in **Figure 5D**, **5E**, the risks of death and disease progression were higher in the H-CSTF2 group. The above results indicate that high CSTF2 level is a key factor that promotes LC progression and increases the risk of recurrence and death in LC patients.

CSTF2 could effectively promote tumor cells proliferation

The proliferative activity of Hep-3B cells is of great significance in promoting LC progression. Firstly, we examined the CSTF2 level in

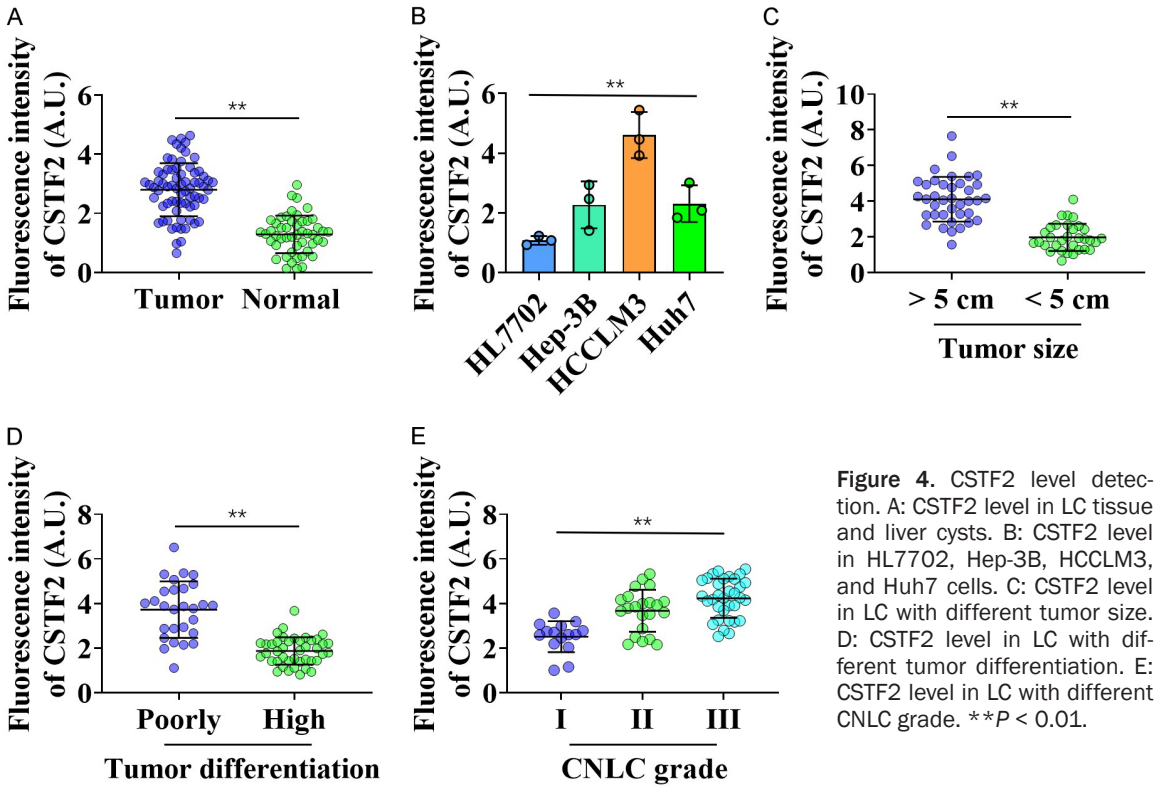

Figure 4. CSTF2 level detection. A: CSTF2 level in LC tissue and liver cysts. B: CSTF2 level in HL7702, Hep-3B, HCCLM3, and Huh7 cells. C: CSTF2 level in LC with different tumor size. D: CSTF2 level in LC with different tumor differentiation. E: CSTF2 level in LC with different CNLC grade. $^{**}P < 0.01$.

Table 1. Relationship between CSTF2 and clinicopathological features

Index		L-CSTF2 group (n=32)	H-CSTF2 group (n=38)	χ^2	*P*
Age	≥ 50	21 (65.62)	21 (55.26)	0.777	0.378
	< 50	11 (34.38)	17 (44.74)		
Tumor diameter (cm)	≥ 5	13 (40.63)	25 (65.79)	4.433	0.035
	< 5	19 (59.37)	13 (34.21)		
Lymph node metastasis	Yes	14 (43.75)	27 (71.05)	5.337	0.021
	No	18 (56.25)	11 (28.95)		
CNLC staging	III	9 (28.13)	24 (63.16)	8.556	0.003
	I+II	23 (71.87)	14 (36.84)		
Tumor differentiation	Poor	8 (25.00)	20 (52.63)	5.526	0.019
	High	24 (75.00)	18 (47.37)		

Table 2. Detection of AFP, CA-199, and PIVKA-II, M (P_{25}, P_{75})

Group	Cases	AFP (ng/mL)	CA-199 (U/L)	PIVKA-II (mAU/mL)
L-CSTF2 group	32	517.13 (18.45, 1123.56)	61.35 (9.13, 287.98)	467.43 (49.65, 2945.63)
H-CSTF2 group	38	588.34 (19.29, 3358.12)	83.34 (10.29, 512.38)	583.75 (40.67, 3721.25)
t		-2.193	-2.886	-2.985
P		0.032	0.005	0.004

all groups of cells and found that the level in L-CSTF2 group was markedly lower than that in H-CSTF2 and control groups, especially in H-CSTF2 group, suggesting that we had successfully performed the transfection experiment (**Figure 6A**). Meanwhile, in comparison to the L-CSTF2 group, the cell connectivity was notably tighter and the proliferation was higher in the control and H-CSTF2 groups, especially in the H-CSTF2 group (**Figure 6B-E**). By labeling

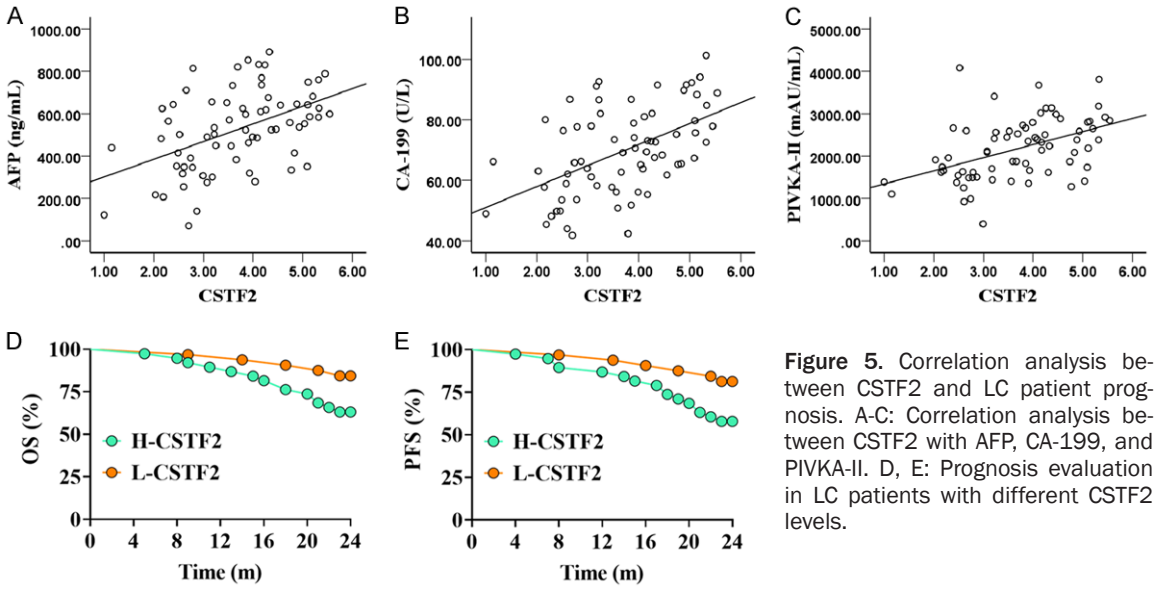

Figure 5. Correlation analysis between CSTF2 and LC patient prognosis. A-C: Correlation analysis between CSTF2 with AFP, CA-199, and PIVKA-II. D, E: Prognosis evaluation in LC patients with different CSTF2 levels.

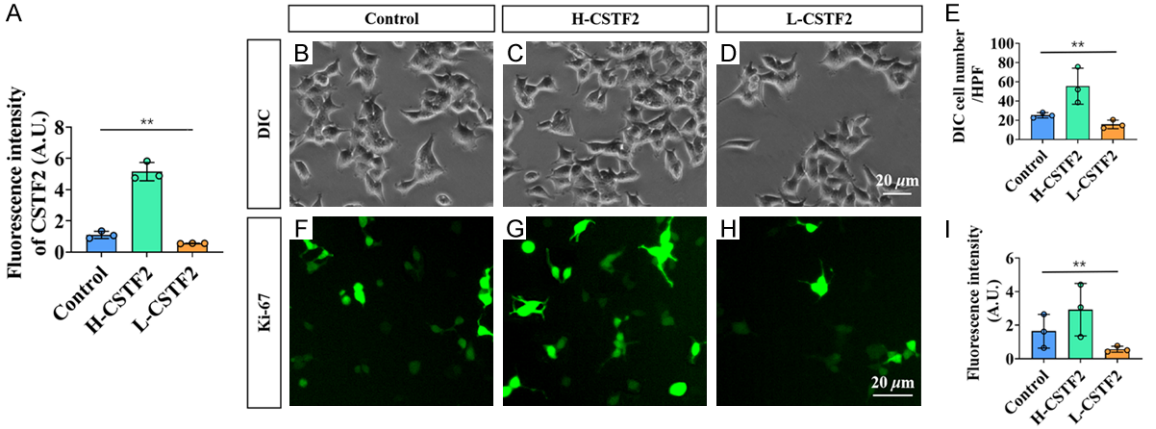

Figure 6. Hep-3B cell growth and proliferation assessment. A: Detection of CSTF2 levels in Hep-3B cells after transfection. B: DIC image of untreated Hep-3B cells, 20×. C: DIC image of Hep-3B cells with CSTF2 over-expression. D: DIC image of Hep-3B cells with CSTF2 silencing. E: Quantitative analysis of transfected Hep-3B cell number per HPF under DIC image. F: anti-Ki67 expression pattern in Hep-3B cells without treatment. G: anti-Ki67 expression pattern in Hep-3B cells with CSTF2 over-expression. H: anti-Ki67 expression pattern in Hep-3B cells with CSTF2 silencing. I: Quantitative fluorescence evaluation of active cells. $^{**}P < 0.01$.

with Ki-67, it was found that the fluorescence intensity of viable Hep-3B cells was elevated in the control and H-CSTF2 groups when compared to that in the L-CSTF2 group, with a more pronounced effect observed in H-CSTF2 group (**Figure 6F-I**). It is indicated that CSTF2 can effectively promote Hep-3B cell proliferation.

CSTF2 could effectively inhibit tumor cells apoptosis

The apoptosis of tumor cells can reflect the inactivation effect of CSTF2 on tumor cells. By labeling apoptotic Hep-3B cells with cleaved caspase-3, more apoptotic cells were observed in both the control and L-CSTF2 groups than in the H-CSTF2 group, with the a more prominent result noted in the L-CSTF2 group (**Figure 7A-C**). Quantitative analysis showed that the fluorescence intensity was the lowest in the H-CSTF2 group (**Figure 7D**). It is indicated that CSTF2 can inhibit tumor cells apoptosis.

CSTF2 could effectively promote tumor cells migration

The migration ability of tumor cells can effectively reflect their invasiveness. Compared to the L-CSTF2 group, more Hep-3B cells migrated into the scratched area in the control group

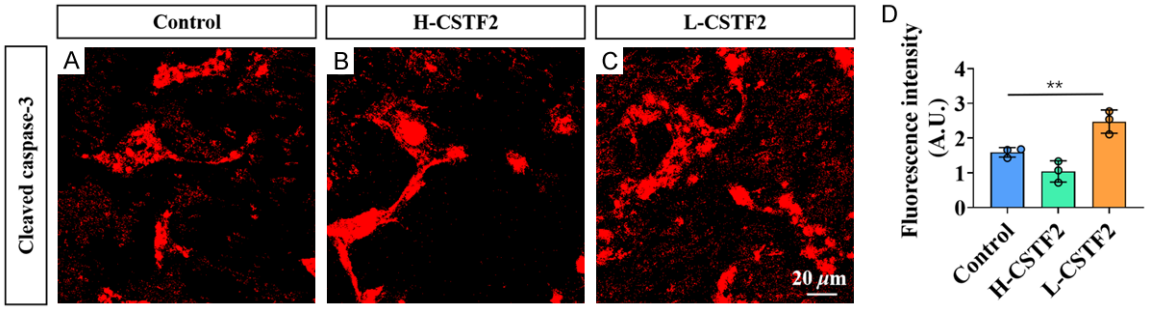

Figure 7. Hep-3B cells apoptosis detection. A: anti-cleaved caspase 3 expression pattern in the control group, 20×. B: anti-cleaved caspase 3 expression pattern in the H-CSTF2 group. C: anti-cleaved caspase 3 expression pattern in the L-CSTF2 group. D: Quantitative fluorescence evaluation of apoptotic cells. $**P < 0.01$.

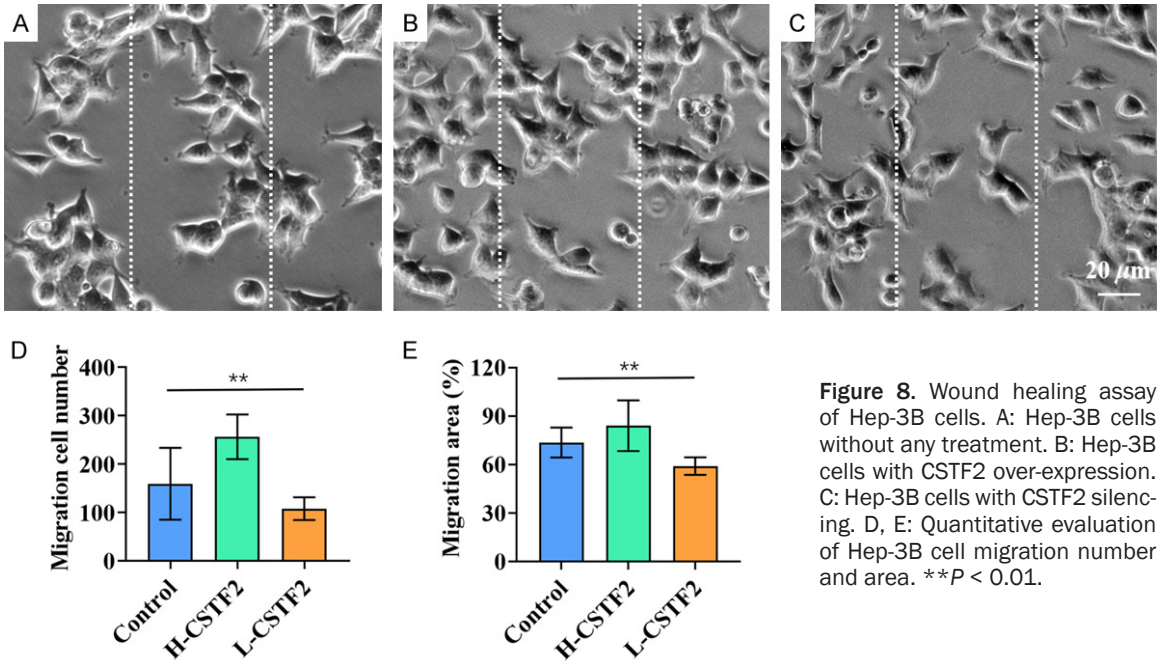

Figure 8. Wound healing assay of Hep-3B cells. A: Hep-3B cells without any treatment. B: Hep-3B cells with CSTF2 over-expression. C: Hep-3B cells with CSTF2 silencing. D, E: Quantitative evaluation of Hep-3B cell migration number and area. $**P < 0.01$.

and the H-CSTF2 group, especially in the H-CSTF2 group (**Figure 8A-C**). The quantitative evaluation of migration cell number and area also showed the same results (**Figure 8D**, **8E**). Therefore, it is indicated that CSTF2 can effectively promote the migration ability of Hep-3B cells.

High CSTF2 level could promote LC progression in mice model

For further confirming the function of CSTF2 on the development of LC, we carried out experiments in mouse models. As shown in **Figure 9A-D**, the CSTF-2 level in H-CSTF2 group exhibited a more significant increase compared to that in the control and L-CSTF2 groups. This indicates successful establishment of LC mouse models with both high and low CSTF2 levels. Meanwhile, the tumor volume and weight of LC mice in the control group and the H-CSTF2 group exhibited more rapid growth compared those in the L-CSTF2 group, especially in the H-CSTF2 group (**Figure 9E-G**).

CSTF2 promotes LC progression through PI3K/AKT/mTOR signaling pathway

As shown in **Figure 10**, compared with those in the L-CSTF2 group, the fluorescence intensity of PI3K, Akt, and mTOR were significantly higher in the control group and the H-CSTF2 group, especially in the H-CSTF2 group. Therefore, PI3K/Akt/mTOR pathway plays a significant role in facilitating CSTF2-driven progression of LC.

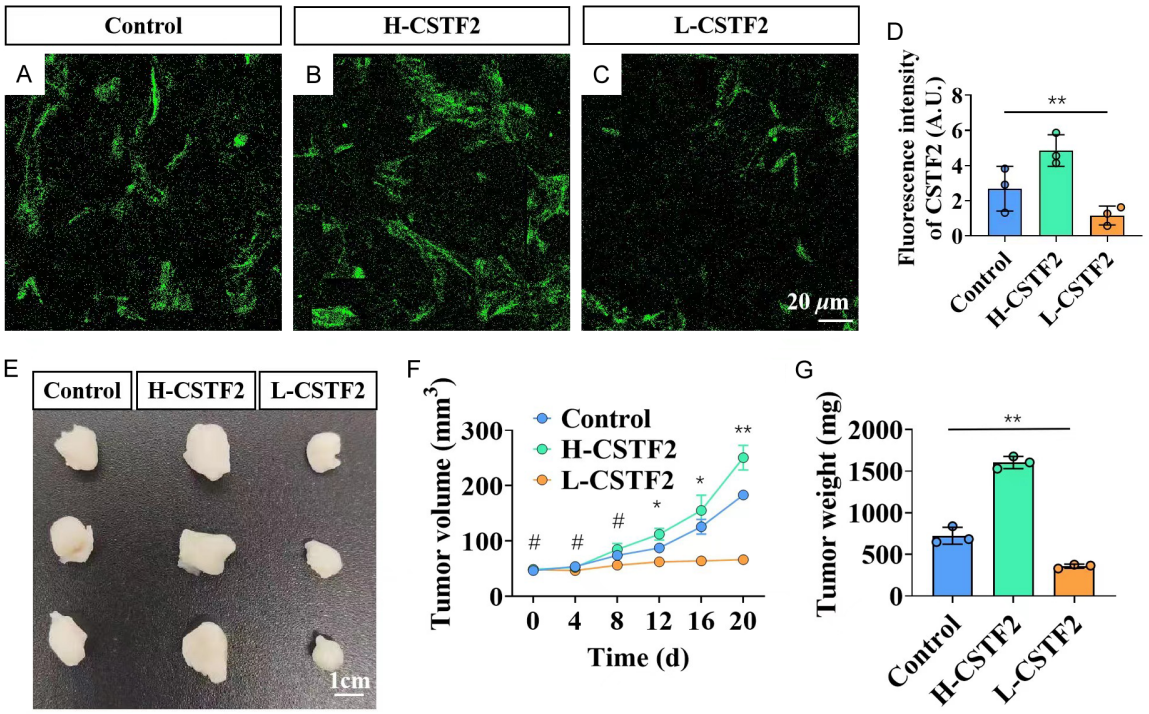

Figure 9. Carcinogenic effect of CSTF2 on LC. A-C: anti-Ki67 expression pattern in LC mice in the control, H-CSTF2, and L-CSTF2 groups, 20×. D: Quantitative evaluation of CSTF2 level. E: Macroscopic appearance of tumor tissue in LC mice in the control, H-CSTF2, and L-CSTF2 groups. F: Comparison of tumor volume in the control, H-CSTF2, and L-CSTF2 groups. G: Comparison of tumor weight in the control, H-CSTF2, and L-CSTF2 groups. #$P > 0.05$, *$P < 0.05$, **$P < 0.01$.

Discussion

Based on statistical data, liver cancer ranked as the third leading cause of mortality among all malignant tumors in 2020 [17]. At present, some progress has been made in LC treatment, such as radiofrequency ablation, surgical resection, and targeted therapy [18], but the choice of treatment methods and clinical efficacy are closely related to the stage of LC. Therefore, improving the early diagnosis rate of LC is crucial in improving the clinical efficacy [19]. In addition, in view of the rapid progression of LC, finding effective targets to inhibit its rapid proliferation is the key to reduce patients' mortality. As a group of DNA sequences closely related to human carcinogenesis, the activation of oncogenes is an important reason for the increased invasiveness of tumor. Some studies have shown that CSTF2 is associated with the modification of oncogene 3'-UTR, leading to its shortening and subsequent activation of the oncogene [20]. For example, CSTF2 was overexpressed in NSCLC cells, and could promote NSCLC progression via shortening the length of cancer-related gene 3'-UTR [21]. Therefore, CSTF2 could be potential sensitive biomarker for the diagnosis of LC, and its correlation with LC is worthy of studying.

To detect the CSTF2 level in LC tissue more efficiently, we innovatively designed a nanostructured DNA probe that can specifically bind to the gene sequence of CSTF2, which can reflect its concentration through fluorescence intensity. This nanostructured DNA probe has several characteristics. Firstly, it can detect target sequence in situ in cells and tissues without amplification, which simplifies the experimental process and saves time. Secondly, by designing nanostructured DNA probes carrying different target groups, the levels of multiple targets in the same tissue can be detected at the same time, thus effectively avoiding multiple experimental procedures because of tissue heterogeneity. Thirdly, it can realize the quantitative analysis of the target by recording the fluorescence intensity, and provide more intuitive visual results for the research. Fourthly, by combining with TiO_2 NP, its permeability in LC

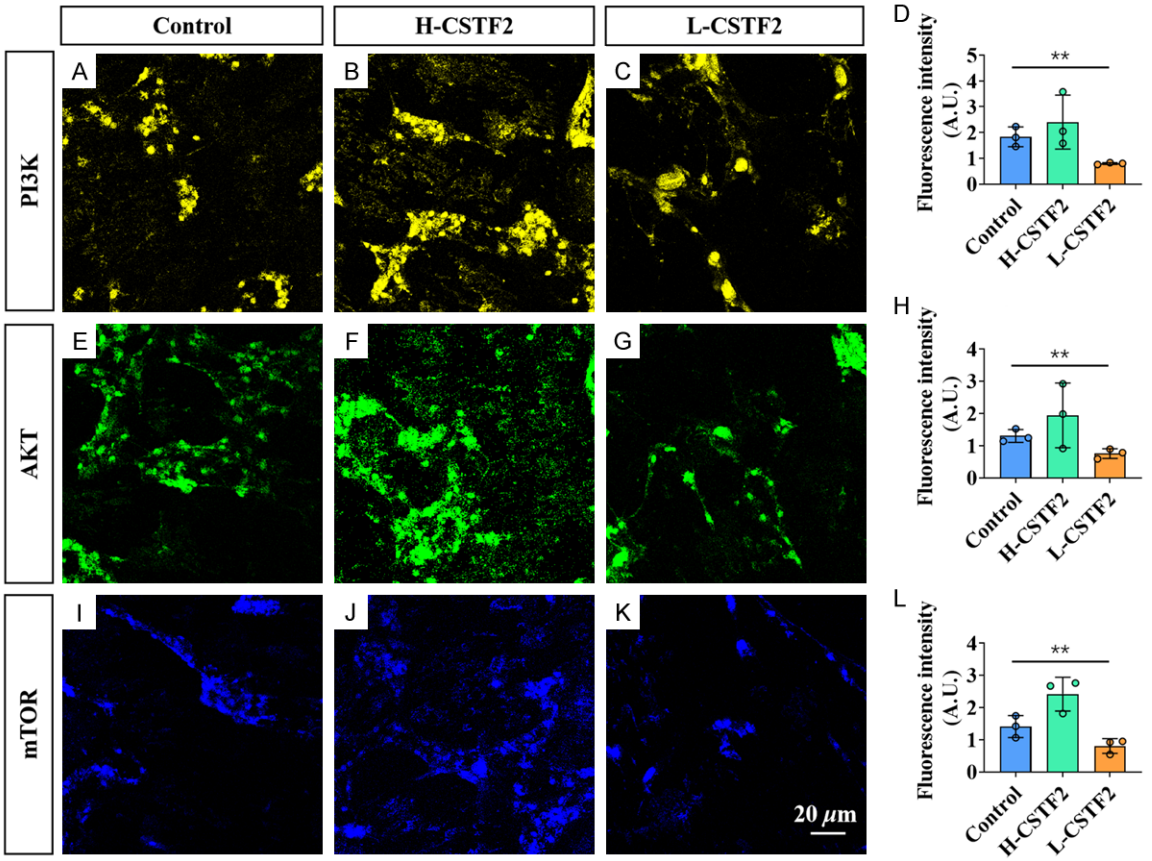

Figure 10. Mechanism of CSTF2 carcinogenesis. A-C: Expressions of PI3K in the control, H-CSTF2, and L-CSTF2 groups. D: Quantitative fluorescence evaluation of PI3K. E-G: Expressions of AKT in the control, H-CSTF2, and L-CSTF2 groups. H: Quantitative fluorescence evaluation of AKT. I-K: Expressions of mTOR in the control, H-CSTF2, and L-CSTF2 groups. L: Quantitative fluorescence evaluation of mTOR. $^{**}P < 0.01$.

tissue and cells is significantly improved, thus further enhancing the accuracy of detection. During the study, we compared the sensitivity and specificity of the nano DNA probe with those of PCR. PCR was performed in all tumor samples to detect CSTF2 expression, and positive results were revealed in 5 samples. Using our DNA probe, high intensity fluorescence was detected in 4 samples, which means the DAN probe has similar results to PCR.

By using the nanostructured DNA probe, we detected significantly increased CSTF2 level in LC tissue and cells. Moreover, the lesions of LC patients with high CSTF2 level were more likely to metastasize, with worse tumor differentiation and lower CNLC stage. In addition, we found that levels of tumor markers increased significantly in the H-CSTF2 group and were significantly positively correlated with the CSTF2 level, resulting in a significant increasing risk of death and disease progression. Chen et al. [22], found that CSTF2 level was higher in bladder cancer patients with higher TNM stage and larger tumor diameter, and those patients were more likely to experience disease progression, which is consistent with our results. To further explore the role of CSTF2 in LC progression, we carried out cell experiments. The results showed that when CSTF2 was overexpressed, the activity of Hep-3B cells increased significantly, and they were more prone to invasion and metastasis, which accelerated LC progression and led to poor prognosis.

To explore the mechanism of CSTF2 promoting LC progression, we established LC mouse models and found that the levels of PI3K, Akt, and mTOR increased significantly in the H-CSTF2 group. PI3K/AKT/mTOR pathway has been found to be involved in the development of a variety of cancers, such as esophageal squa-

mous cell carcinoma, ovarian cancer, and gastrointestinal stromal tumors [23-25]. In addition, Xue et al. [26] found that Anemoside B4 realized an anticancer effect in LC by inactivating PI3K/Akt/mTOR pathway. On the contrary, the proliferation and migration of LC cells could be enhanced by activating PI3K/AKT/mTOR pathway [27]. Our results showed that high CSTF2 levels could activate PI3K/AKT/mTOR pathway, thus increasing the volume and weight of tumors in LC mouse model. Therefore, CSTF2 can be used as an early biomarker of LC and a novel potential target for the treatment.

Conclusion

In this study, the designed nano-TiO_2-DNA probe enables rapid in-situ detection of CSTF2 in puncture samples from LC patients, offering high sensitivity and specificity, which eliminates the need for DNA extraction or PCR procedures. Using this detection method, we find that CSTF2 level is significantly increased in LC tissue and cell lines, and is closely related to the poor prognosis of LC patients. In addition, CSTF2 can increase the proliferative activity and invasiveness of LC cells through PI3K/AKT/mTOR signaling pathway, so as to play a carcinogenic role.

Acknowledgements

This study was supported by grant from National Natural Science Foundation of China (Grant No. 82272880), Tianjin Science and Technology Plan Project (Grant No. 22ZYQYSY00030), Tianjin Health Technology Project (TJWJ2022XK041, TJWJ2022XK042, TJWJ2022XK043, TJWJ2023MS053), Bethune Charity Foundation Project (B-0307-H20200302), and funded by Tianjin Key Medical Discipline (Specialty) Construction Project (TJYXZDXK-062B, TJYXZDXK-079D) and Qinghai Province "Kunlun Talents·Advanced Innovation and Entrepreneurship Talents" Project.

Disclosure of conflict of interest

None.

Address correspondence to: Wei Meng, High Altitude Characteristic Medical Research Institute, Huangnan Tibetan Autonomous Prefecture People's Hospital, Huangnan 811399, Qinghai, P. R. China. Tel: +86-0973-8722474; E-mail: mwei7178@163.com; Zhijiang Shao, Department of General Surgery, Tianjin Fifth Central Hospital, Tianjin 300450, P. R. China. Tel: +86-022-65665000; E-mail: shzhj315@126.com

References

[1] Akman HB, Oyken M, Tuncer T, Can T and Erson-Bensan AE. 3'UTR shortening and EGF signaling: implications for breast cancer. Hum Mol Genet 2015; 24: 6910-6920.

[2] Aragaki M, Takahashi K, Akiyama H, Tsuchiya E, Kondo S, Nakamura Y and Daigo Y. Characterization of a cleavage stimulation factor, 3' pre-RNA, subunit 2, 64 kDa (CSTF2) as a therapeutic target for lung cancer. Clin Cancer Res 2011; 17: 5889-5900.

[3] Cao W, Chen HD, Yu YW, Li N and Chen WQ. Changing profiles of cancer burden worldwide and in China: a secondary analysis of the global cancer statistics 2020. Chin Med J (Engl) 2021; 134: 783-791.

[4] Chen JG and Zhang SW. Liver cancer epidemic in China: past, present and future. Semin Cancer Biol 2011; 21: 59-69.

[5] Chen X, Zhang JX, Luo JH, Wu S, Yuan GJ, Ma NF, Feng Y, Cai MY, Chen RX, Lu J, Jiang LJ, Chen JW, Jin XH, Liu HL, Chen W, Guan XY, Kang TB, Zhou FJ and Xie D. CSTF2-induced shortening of the RAC1 3'UTR promotes the pathogenesis of urothelial carcinoma of the bladder. Cancer Res 2018; 78: 5848-5862.

[6] Duan Y, Haybaeck J and Yang Z. Therapeutic potential of PI3K/AKT/mTOR pathway in gastrointestinal stromal tumors: rationale and progress. Cancers (Basel) 2020; 12: 2972.

[7] Ediriweera MK, Tennekoon KH and Samarakoon SR. Role of the PI3K/AKT/mTOR signaling pathway in ovarian cancer: biological and therapeutic significance. Semin Cancer Biol 2019; 59: 147-160.

[8] Frau M, Feo F and Pascale RM. Pleiotropic effects of methionine adenosyltransferases deregulation as determinants of liver cancer progression and prognosis. J Hepatol 2013; 59: 830-841.

[9] Huang C and Xie K. Crosstalk of Sp1 and Stat3 signaling in pancreatic cancer pathogenesis. Cytokine Growth Factor Rev 2012; 23: 25-35.

[10] Lembo A, Di Cunto F and Provero P. Shortening of 3'UTRs correlates with poor prognosis in breast and lung cancer. PLoS One 2012; 7: e31129.

[11] Li MZ, Wang JJ, Yang SB, Li WF, Xiao LB, He YL and Song XM. ZEB2 promotes tumor metastasis and correlates with poor prognosis of human colorectal cancer. Am J Transl Res 2017; 9: 2838-2851.

[12] Morris AR, Bos A, Diosdado B, Rooijers K, Elkon R, Bolijn AS, Carvalho B, Meijer GA and Agami R. Alternative cleavage and polyadenyl-

ation during colorectal cancer development. Clin Cancer Res 2012; 18: 5256-5266.
[13] Omata M, Lesmana LA, Tateishi R, Chen PJ, Lin SM, Yoshida H, Kudo M, Lee JM, Choi BI, Poon RT, Shiina S, Cheng AL, Jia JD, Obi S, Han KH, Jafri W, Chow P, Lim SG, Chawla YK, Budihusodo U, Gani RA, Lesmana CR, Putranto TA, Liaw YF and Sarin SK. Asian Pacific Association for the Study of the Liver consensus recommendations on hepatocellular carcinoma. Hepatol Int 2010; 4: 439-474.
[14] Shiani A, Narayanan S, Pena L and Friedman M. The role of diagnosis and treatment of underlying liver disease for the prognosis of primary liver cancer. Cancer Control 2017; 24: 1073274817729240.
[15] Sia D, Villanueva A, Friedman SL and Llovet JM. Liver cancer cell of origin, molecular class, and effects on patient prognosis. Gastroenterology 2017; 152: 745-761.
[16] Song XZ, Ren XN, Xu XJ, Ruan XX, Wang YL and Yao TT. LncRNA RHPN1-AS1 promotes cell proliferation, migration and invasion through targeting miR-7-5p and activating PI3K/AKT/mTOR pathway in hepatocellular carcinoma. Technol Cancer Res Treat 2020; 19: 1533033820957023.
[17] Wongfieng W, Jumnainsong A, Chamgramol Y, Sripa B and Leelayuwat C. 5'-UTR and 3'-UTR regulation of MICB expression in human cancer cells by novel microRNAs. Genes (Basel) 2017; 8: 213.
[18] Wu N, Du Z, Zhu Y, Song Y, Pang L and Chen Z. The expression and prognostic impact of the PI3K/AKT/mTOR signaling pathway in advanced esophageal squamous cell carcinoma. Technol Cancer Res Treat 2018; 17: 1533033818758772.
[19] Xia Z, Donehower LA, Cooper TA, Neilson JR, Wheeler DA, Wagner EJ and Li W. Dynamic analyses of alternative polyadenylation from RNA-seq reveal a 3'-UTR landscape across seven tumour types. Nat Commun 2014; 5: 5274.
[20] Xie J, Pan X, Wang M, Ma J, Fei Y, Wang PN and Mi L. The role of surface modification for TiO2 nanoparticles in cancer cells. Colloids Surf B Biointerfaces 2016; 143: 148-155.
[21] Xue S, Zhou Y, Zhang J, Xiang Z, Liu Y, Miao T, Liu G, Liu B, Liu X, Shen L, Zhang Z, Li M and Miao Q. Anemoside B4 exerts anti-cancer effect by inducing apoptosis and autophagy through inhibiton of PI3K/Akt/mTOR pathway in hepatocellular carcinoma. Am J Transl Res 2019; 11: 2580-2589.
[22] Yang M, Xiao X, Xing X, Li X, Xia T and Long H. KRAS and VEGF gene 3'-UTR single nucleotide polymorphisms predicted susceptibility in colorectal cancer. PLoS One 2017; 12: e0174140.
[23] Zhang MH and Liu J. Cleavage stimulation factor 2 promotes malignant progression of liver hepatocellular carcinoma by activating phosphatidylinositol 3'-kinase/protein kinase B/mammalian target of rapamycin pathway. Bioengineered 2022; 13: 10047-10060.
[24] Zhang S, Zhang X, Lei W, Liang J, Xu Y, Liu H and Ma S. Genome-wide profiling reveals alternative polyadenylation of mRNA in human non-small cell lung cancer. J Transl Med 2019; 17: 257.
[25] Zuo M and Huang J. The history of interventional therapy for liver cancer in China. J Interv Med 2019; 1: 70-76.
[26] Zuo TT, Zheng RS, Zhang SW, Zeng HM and Chen WQ. Incidence and mortality of liver cancer in China in 2011. Chin J Cancer 2015; 34: 508-513.
[27] Cesmeli S and Biray Avci C. Application of titanium dioxide (TiO(2)) nanoparticles in cancer therapies. J Drug Target 2019; 27: 762-766.